Desalination and Water Treatment
www.deswater.com
doi: 10.5004/dwt.2021.26868

219 (2021) 303–311
April

Application of artificial intelligence technology in removal of heavy metals from water by iron oxide

Xiaofa Zheng[a,*], Li Yang[b], Zhonghui Lin[c]

[a]*Admission and Employment Office, Chongqing Vocational and Technical University of Mechatronics, Chongqing 402760, China, email: cqzxf2020@163.com*
[b]*School of Business Administration, Chongqing Vocational and Technical University of Mechatronics, Chongqing 402760, China, email: cqyl_2020@163.com*
[c]*Computer and Art Media Branch, Heilongjiang Agricultural Reclamation Vocational College, Haerbin 150025, China, email: wwslyt@163.com*

Received 15 August 2020; Accepted 23 November 2020

ABSTRACT

Heavy metal pollution is even more harmful to human health. This paper studies the application of artificial intelligence technology in the removal of heavy metals from water by iron oxides. PBTCA and th-904 molecules are adsorbed on the surface of nanoparticles to form a layer of polymer protective film, which surrounds the nanoparticles, effectively preventing the formation of nano zero-valent iron aggregates. nZVI-Fe_3O_4/ACF composites were prepared. The experimental results show that the adsorption kinetic model of the composite material conforms to the pseudo-second-order reaction adsorption rate model. With the increase of pH value, the adsorption percentage of Cd(II) and Pb(II) increases, and the adsorption percentage of Cd(II) tends to balance within 120 min, reaching 99.25%, 0037 mg/L, meeting the World Health Organization (WTO) standard for Cd(II) in drinking water (0.005 mg/L).

Keywords: Iron oxide; Water; Heavy metal; Artificial intelligence

1. Introduction

The importance of heavy metals in industrial production makes them very widely used. However, the untreated or incomplete heavy metal pollutants discharged into the environment will cause serious consequences to soil and water. Moreover, when the amount of heavy metals exceeds a certain value, it will cause harm to the organism [1]. Heavy metal pollutants mainly include mercury, cadmium, lead, copper, chromium, nickel, iron, manganese, zinc, etc. Although arsenic is not heavy metal, its behavior, source, and harm are similar to those of heavy metals, so it is usually included in the category of heavy metals for discussion [2]. As far as the needs of plants are concerned, they can be divided into two categories: one is the elements that are not needed for plant growth and development but are more harmful to human health, such as chromium, mercury, lead, arsenic, cadmium, etc., the other is the elements required for the normal growth and development of plants, and have certain physiological functions to the human body, such as copper and zinc, but too much will cause pollution and hinder the growth and development of plants. Heavy metals will not degrade and disappear in the environment, but transfer between different circles through migration and transformation. Once the products are enriched and enter the human body through the food chain, it will cause greater harm to human health.

* Corresponding author.

The remediation technology of cadmium pollution in water body mainly includes precipitation method, ion exchange, and membrane separation. Precipitation method generally deals with water with high cadmium concentration, and the commonly used precipitants are sulfide, hydroxide, and iron oxide [3]. When the precipitation method is applied, the precipitate particles formed are too fine, which makes the solid–liquid separation difficult. At the same time, when there is complexing agent in the water, it will inhibit the precipitation of Cd. When ion-exchange method and membrane separation technology are applied, the treatment effect is good, but the cleaning cost of resin and membrane is high, so it is difficult to be applied on a large scale [4]. At present, there are many researches on the bioremediation of heavy metal pollution in the water body at home and abroad. Through the special enrichment and degradation ability of heavy metal elements or organic substances by plants, pollutants in the environment can be removed, or the toxicity of pollutants can be eliminated, so as to achieve the purpose of pollution control and ecological restoration.

Iron-based materials, including iron (hydrogen) oxides and zero-valent iron, can repair a variety of environmental pollutants. Iron (hydrogen) oxides, especially hematite and goethite, widely exist in soil and sediment, and have good adsorption properties for heavy metals in the environment, and have been used as one of the important materials for the treatment of heavy metal pollutants for many years [5]. At present, there are many methods to treat heavy metal wastewater. Among them, nano zero-valent iron (nZVI) is widely used in the treatment of heavy metal in water due to its large specific surface area and high reaction activity. However, iron oxide passivation layer will be formed on the surface of nano-sized zero-valent iron during the reaction process, which will inhibit its reaction activity. Therefore, the solution of surface passivation will determine its further engineering application. In order to improve the physical and chemical properties of nano iron oxide materials, improve the stability, dispersion, and affinity of nano iron oxide materials, so as to improve the adsorption capacity of nano iron oxide and promote the engineering application of nano iron oxide materials.

In this paper, artificial intelligence technology is applied to the preparation of nano zero-valent iron to reduce the passivation layer of iron oxide. In this paper, the typical toxic, easy to accumulate in the environment and cause serious harm to the environment and health of hexavalent chromium and cadmium as the main research object, based on the nano zero-valent iron technology, to treat the water polluted by heavy metals, to solve the problem of iron nanoparticles easy to oxidize and agglomerate [6].

2. Artificial intelligence technology enhances the agglomeration of iron oxide particles

After the advent of computers, human beings began to have a tool to simulate human thinking. In the years to come, countless scientists worked hard for this goal. Nowadays, artificial intelligence is no longer the patent of several scientists. There are people studying this subject in the computer departments of almost all universities in the world. College students learning computer must also learn such a course. With the unremitting efforts of all, computers seem to have become very smart [7].

In this paper, composite materials were prepared under intelligent equipment, and the surface modification of nano iron oxide was carried out, so as to improve the physical and chemical properties of nano iron oxide materials, improve the stability, dispersion, and affinity of nano iron oxide materials. According to the intelligent equipment, experimental research is carried out.

Due to the large specific surface area of nano iron oxide materials, it is easy to agglomerate in water, which limits the surface activity of nano iron oxide materials, resulting in the performance of materials cannot be fully played. In addition, the interaction of various substances in water will also affect the adsorption of heavy metal ions by nano iron oxides, such as competitive adsorption of heavy metal ions in phosphate turn [8]. In order to improve the physical and chemical properties of nano iron oxide materials, improve the stability, dispersion, and affinity of nano iron oxide materials, so as to improve the adsorption capacity of nano iron oxide and promote the engineering application of nano iron oxide materials.

The study on the reusability of adsorbent is the regeneration process of adsorbent, and the adsorption capacity of adsorbent can be regained by selecting appropriate eluent [9]. The molecular structure of PBTCA is shown in Fig. 1. Each PBTCA molecular structure contains three – COOH and one PO_3H_2; and th-904 is a polycarboxylic acid polymer, which contains multiple – COOH groups, so it can play a role in the dispersion of nano zero-valent iron.

First, PBTCA and th-904 and the molecules adsorb on the surface of nanoparticles to form a protective polymer film, which surrounds the nanoparticles. This shell increases the closest distance between the two particles and reduces the interaction of van der Waals force, so that the dispersion system can be stabilized. Secondly, a large number of groups with the same charge (negative charge) are generated after hydrolysis, which changes the surface charge distribution of the particles. It plays an important role in increasing the removal of heavy metal pollutants.

In order to inhibit further oxidation, iron nanoparticles can be coated with self-generated iron oxide, and the surface modification of iron nanoparticles can also be carried out. In order to prevent the agglomeration of nanoparticles,

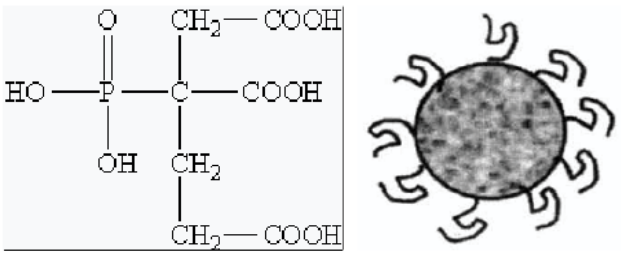

Fig. 1. Molecular structure formula of PBTCA and schematic diagram of iron nanoparticles after surface adsorption of dispersant.

polymers or surfactants can be used as stabilizers to reduce the agglomeration degree of nanoparticles.

3. Removal of heavy metals from water by ferric oxide

3.1. Removal mechanism of heavy metal ions by iron oxides

The adsorption strength of metal oxides is determined by the charge/radius ratio of metal ions, the electronegativity of metal ions, and the protonation degree of hydroxyl groups on the surface of oxides. The particle surface characteristics are important factors affecting adsorption characteristics [10]. The reaction mechanism of removing heavy metal ions is as shown in Fig. 2.

In an aqueous solution, there are many active sites and functional groups on the surface of iron oxide, and there are many forms of specific adsorption with metal ions, such as the formation of coordination bond, isomorphic replacement, ion exchange, surface complexation, hydrolysis on the surface of metal (hydrogen) oxide, and so on [11]. Langmuir adsorption isotherm model is expressed as follows:

$$\frac{C_e}{q_e} = \frac{C_e}{q_m} + \frac{1}{K_L q_m} \tag{1}$$

In the above formula, q_e is the equilibrium absorption capacity, mg/g, q_m is the maximum adsorption capacity of unit absorbent, mg/g, C_e is the concentration of metal ions in the solution at equilibrium, mg/L, K_L is the adsorption coefficient, its size depends on the temperature and the adsorption heat of the material, and its size reflects the binding force between the adsorbate and the adsorbent, L/mg.

Adsorption kinetics is to study the adsorption rate and explore various factors affecting the rate. The study of adsorption kinetics mainly monitors the experimental conditions affecting the adsorption rate, obtains the adsorption equilibrium time, establishes the adsorption kinetic model, and calculates the kinetic parameters, so as to provide information on the mechanism of the adsorption process [12].

The study of the adsorption process and time, as well as the relationship between them, is mainly explained by adsorption kinetics, which shows that there is a certain relationship between adsorption rate and dynamic equilibrium [13]. The mass transfer process can be affected by the concentration of adsorbate, temperature, solution foot, adsorbent morphology, and particle size. There are two kinds of adsorption kinetic models, quasi-first-order and quasi-second-order.

The quasi-first-order kinetic equation model can be described by the following equation:

$$\log\left(q_e - q_t\right) = \log q_t - \frac{K_1 t}{2.303} \tag{2}$$

In Eq. (2), q_e is the equilibrium adsorption capacity, mmol/g, q_t is the adsorption amount at t time, mmol/g, K_1 is the quasi-first-order adsorption rate constant, L/min.

The equation expression of pseudo-second-order adsorption kinetics is as follows:

$$\frac{t}{q_t} = \frac{1}{K_2 q_e^2} + \frac{t}{q_e} \tag{3}$$

where K_2 is the pseudo-second-order adsorption rate constant. The effect pictures of the two kinds of fitting curves are shown below.

From Fig. 3, it can be seen that the correlation coefficients of the quasi-second-order adsorption rate model equations are greater than 0.99, which is far better than that of the quasi-first-order adsorption rate model. Moreover, the theoretical adsorption amount calculated by the quasi-second-order rate model equation is in good agreement with the actual adsorption amount, indicating that the adsorption kinetic model conforms to the quasi-second-order reaction adsorption rate model, and the chemical adsorption is taken as the rate in the process control step process.

Surface coating shell often involves surfactants, polymers, precious metals, and transition metals, amorphous Guido dioxide, and graphite, etc. the oxide layer on the surface of iron particles can also be directly used as the coating shell. The method of coating iron nanoparticles with self-generated iron oxide is the most simple and effective

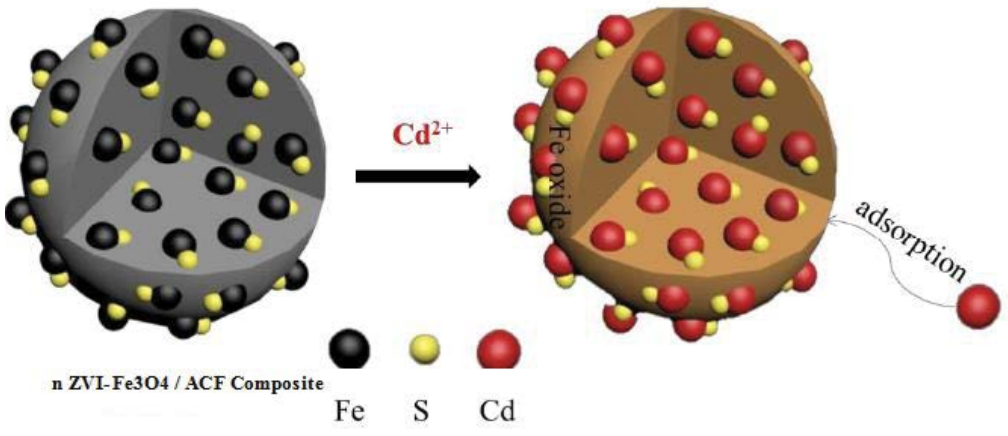

Fig. 2. Schematic diagram of the mechanism of removing heavy metal ions by composite materials.

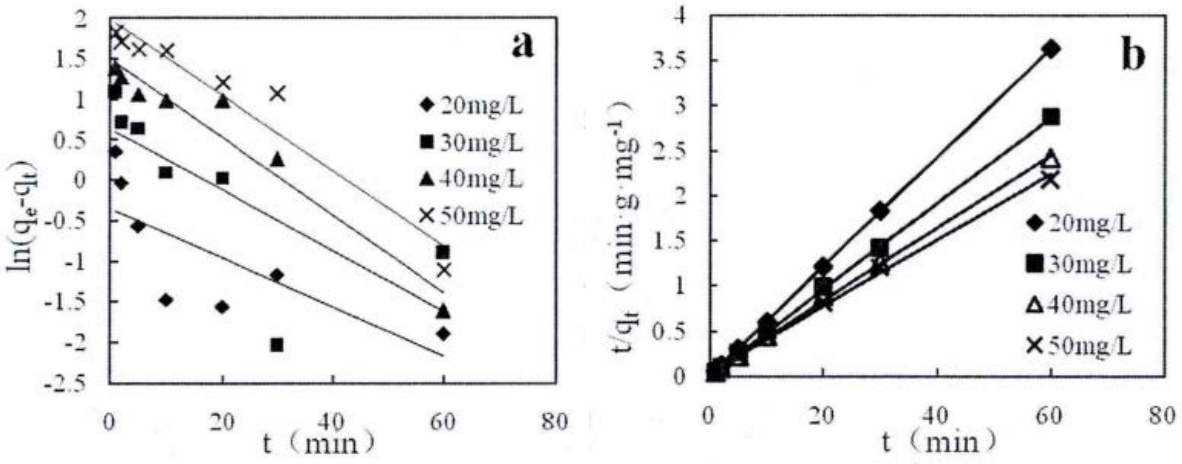

Fig. 3. Linear fitting curve of adsorption rate: (a) quasi-first-order and (b) quasi-second-order adsorption rate..

method, and fully considers the actual situation that the surface iron oxide is difficult to avoid [14]. In addition to oxidation, iron nanoparticles are easy to agglomerate due to their small particle size and large surface energy. They can be generally used as polymer, surfactant, inorganic or organic chemical inert carrier. Montmorillonite is a kind of layered valproate clay mineral. Its structural unit layer is composed of two shoe oxygen tetrahedrons sandwiched with an oxygen octahedron sheet. The interlayer domain is occupied by hydrate cation ions and replaced by equilibrium isomorphism, which can produce a negative charge of the laminar. It has cation exchange property, expansibility, dispersibility, and adsorption. Montmorillonite is used as a carrier and dispersant in zero-valent iron nanoparticles. In the process of preparation, the core-shell structure is formed by surface coating to inhibit further oxidation [15].

The surface modification of nano iron oxide can improve the physical and chemical properties of nano iron oxide material, improve the stability, dispersion, and affinity of nano iron oxide material, and then increase the adsorption capacity of nano iron oxide, and promote the engineering application of nano iron oxide material.

3.2. Preparation of nZVI-Fe_3O_4/ACF composites

The preparation method of nZVI-Fe_3O_4/ACF is shown in Fig. 4. Firstly, 0.304 g $FeCl_3{\cdot}6H_2O$ is dissolved in a flask containing 25 mL ethanol aqueous solution (ethanol:deionized water = 3:7, V/V), and then 0.189 g Fe_3O_4 is added into the solution, and an ultrasonic wave is performed at 40 kW for 20 min to form a solid–liquid mixture [16]. Then 25 mL 0.5 mol/L $NaBH_4$ was added to the mixture at a drop rate of 0.17 mL/S until no significant H_2 was produced. The reaction equation is as follows:

$$4\left(Fe_3O_4 - Fe^{3+}\right) + 3BH_4^- + 9H_2O \rightarrow 4\left(Fe^0Fe_3O_4\right) + 3BO_3^- + 12H^+ + 9H_2\uparrow \quad (4)$$

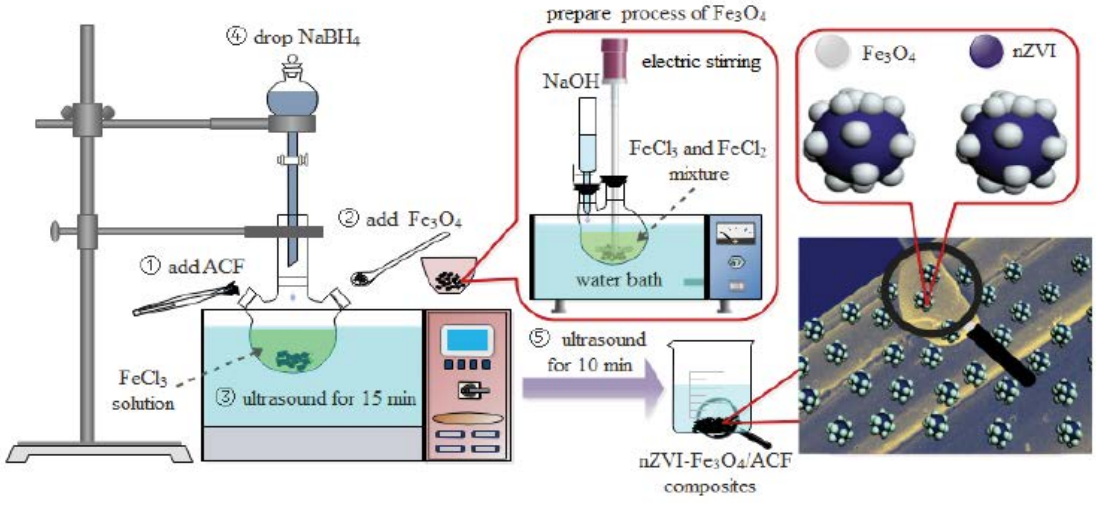

Fig. 4. Preparation of nZVI-Fe_3O_4/ACF composite.

3.2.1. Preparation of activated carbon fiber

ACF was obtained from activated carbon fiber felt and cut into 0.4 cm × 0.4 cm × 0.2 cm sheets with scissors. Then it was soaked in 5% hydrochloric acid for 24 h, then washed with deionized water to be nearly neutral, and dried at 105°C for use.

3.2.2. Preparation of nZVI

nZVI was prepared by reduction of $FeCl_3{\cdot}6H_2O$ with $NaBH_4$. Firstly, 0.304 g of $FeCl_3{\cdot}6H_2O$ was dissolved in a flask containing 25 mL ethanol aqueous solution (ethanol:deionized water = 3:7, V/V), and then 25 mL of 0.5 mol/L $NaBH_4$ was added to the ethanol solution in an ultrasonic environment with a power of 40 kW until no significant H_2 was produced. When the drop rate of $NaBH_4$ is 0.17 mL/s, the prepared nZVI is separated from the aqueous solution by a strong magnet, and then cleaned with absolute ethanol and deionized water for three times. The nZVI prepared in the experiment should be used in the next step of the experiment or stored in a vacuum environment immediately. The reaction equation is as follows:

$$4Fe^{3+} + 3BH_4^- + 9H_2O \rightarrow 4Fe^0 + 3BO_3^- + 12H^+ + 9H_2\uparrow \quad (5)$$

3.2.3. Preparation of Fe_3O_4

According to the existing methods in the laboratory, the cleaned 316 L porous stainless steel tube was placed in a tubular resistance furnace and sintered with a set heating program. The specific sintering procedure is as follows: holding at 110°C for 1 h, holding at 250°C for 2 h, sintering atmosphere (air in the front section and nitrogen in the back section), changing the atmosphere temperature to 400°C, holding at 400°C for 3 h, and finally sintering temperature at 850°C for 3 h. The heating rate of all heating processes is 1°C/min.

3.3. Effect of initial pH of solution

The residual concentration of heavy metals in the solution was determined by flame graphite furnace atomic absorption spectrometry, and the adsorption percentage r (%) was calculated as follows:

$$r = \frac{(C_0 - C_t)}{C_0} \times 100 \quad (6)$$

In Eq. (6), C_0 is the initial mass concentration of Cd(II) and Pb(II) before adsorption, mg/L; C_t is the mass concentration of Cd(II) and Pb(II) at adsorption time t, mg/L.

3.4. Effect of adsorption time on adsorption capacity of heavy metals

The adsorption capacity of q_t (mg/g) was calculated and repeated three times. The calculation formula of adsorption capacity is as follows:

$$q_t = \frac{(C_0 - C_t)V}{m} \quad (7)$$

where V is the volume of solution, L; m is the mass of iron oxide film on 316 L stainless steel, G. In order to solve the problem of iron nanoparticles easy to oxidize and agglomerate.

4. Experiment

4.1. Experimental scheme

The stock solution of Cd(II) and Pb(II) was diluted to 750 mg/L with deionized water, 100 mL of each heavy metal diluent was put into a 150 mL blue cap bottle, and the composite material was added. The composite material was placed in a shaker with a speed of 150 rpm and vibrated at 25°C. Samples were taken at intervals (0, 5, 15, 30, 60, 90, and 120 min) to determine the concentration of Cd in the reaction solution [17].

The concentrations of Cd(II) and Pb(II) in the solution were determined by atomic absorption spectrometry (AAS) (aa-6300c, Shimadzu, Japan), Cd(II) and Pb(II) were determined by inductively coupled plasma-optical emission spectrometry (ICP-OES; optima 8300, Perkin Elmer, USA) and AFS (afs-9130, Ji Tian, China).

The results of the batch experiment were expressed as the mean ± standard deviation of the three experiments. SPSS 19.0 software was used for one-way ANOVA and Duncan method was used for multiple tests (α = 0.05), is as shown in Fig. 5.

4.2. Analysis of experimental results

After the reaction with Cd(II), the HAADF diagram showed that the composite showed irregular flocs, which may be caused by the oxidation and corrosion of nanoparticles during the reaction, is as shown in Fig. 6.

After reacting with Cd(II), Fe, O, s, and Cd are evenly distributed on the whole composite particles. Compared with the composite particles before reaction, more O was detected and its distribution matched with that of Fe [18]. At the same time, the distribution of Cd after reaction overlapped with s, indicating that s provided an active site for the removal of Cd in the reaction process of Cd and composite, and the composite particles were seriously oxidized is as shown in Fig. 7.

It can be seen from Fig. 8 that the characteristic peak of FeO disappears after the reaction with Cd(II), and a strong characteristic peak of γ-FeO(OH) is detected, indicating that nZVI particles are oxidized during the reaction [19].

It can be seen from Fig. 9 that after the reaction of nZVI with Cd(II), the characteristic peak of Fe s disappears, and a strong Raman vibration peak of Cd is detected at 306 cm^{-1}. When the composite reacts with Cd(II), Cd can replace Fe in Fe s to form Cd, and the composite is oxidized to different iron oxides.

It can be seen from Fig. 10 that after the reaction with various heavy metals, the composite materials have formed many agglomerated spherical particles and sheet structure, which may be caused by the different oxidation processes of different metals and composite materials [20].

High concentration and high pH value will make Cd(II) and Pb(II) hydrolyze and precipitate in the aqueous

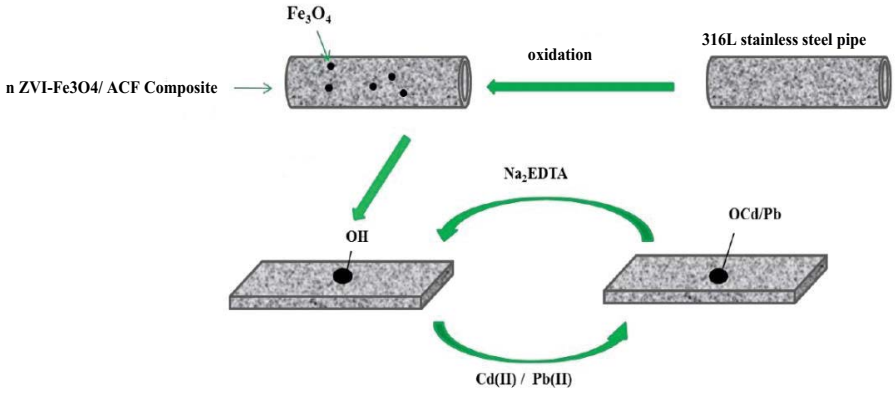

Fig. 5. Schematic diagram of removal of Cd(II) and Pb(II) from aqueous solution by composite materials.

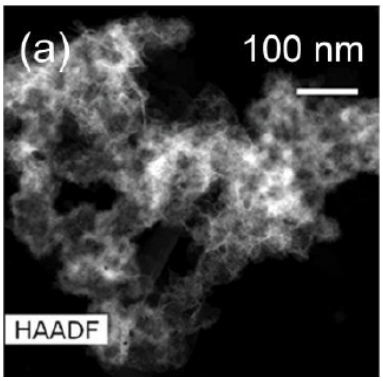

Fig. 6. HAADF after reaction with Cd(II).

solution, resulting in the change of the concentration of heavy metal ions in the solution. Therefore, the initial concentrations of Cd(II) and Pb(II) are set at 1 and 5 mg/L respectively, and the initial pH ranges are 3.0–9.0 and 3.0–6.0, respectively. The effect of the initial pH value of the solution on the adsorption rate of Cd(II) Pb(II) is shown in Fig. 11.

It can be seen from Fig. 11 that the adsorption percentages of Cd(II) and Pb(II) increase with the increase of pH value, which may be due to the competition between hydrogen ions and heavy metal ions in the solution for adsorption sites [21–23]. With the increase of pH in the solution, the concentration of hydrogen ions in the solution decreases, and the competition of hydrogen ions weakens, so that more Cd(II) and Pb(II) are adsorbed on the *in-situ*

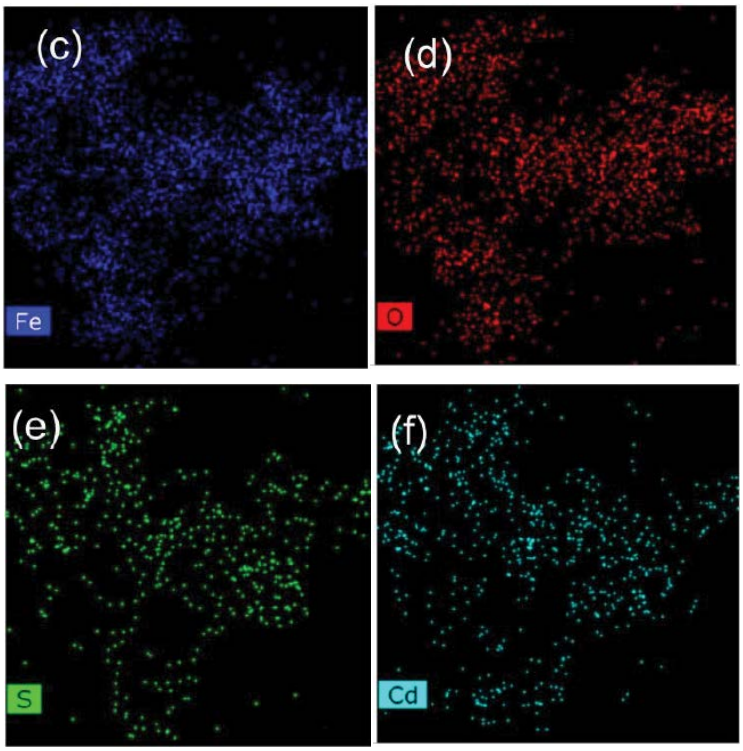

Fig. 7. Comparison of composite particles with (a) Fe, (b) O, (c) s, and (d) Cd reactions.

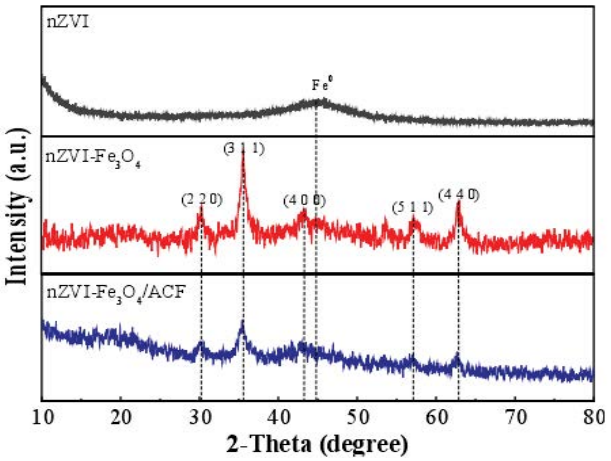

Fig. 8. XRD pattern of the composite.

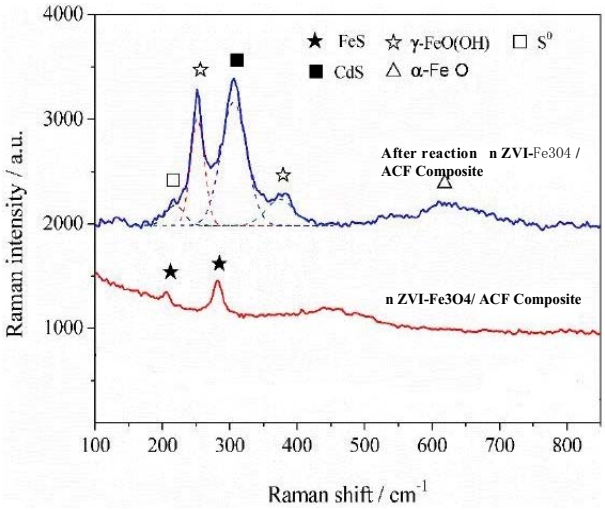

Fig. 9. Raman spectra of the composite before and after reaction with Cd(II).

oxidized Fe_3O_4 membrane, resulting in the increase of adsorption percentage.

It can be seen from Fig. 12 that the adsorption properties of the composite materials for Cd(II) and Pb(II) in drinking water are increased at first and then tend to balance. The adsorption percentage of Cd(II) tends to be balanced within 120 min, reaching 99.25%. The concentration of residual Cd(II) in drinking water after adsorption is 0.0037 mg/L, which conforms to the limit standard of Cd(II) in drinking water (0.005 mg/L) stipulated by the World Health Organization (WTO). The results show that Fe_3O_4 membrane

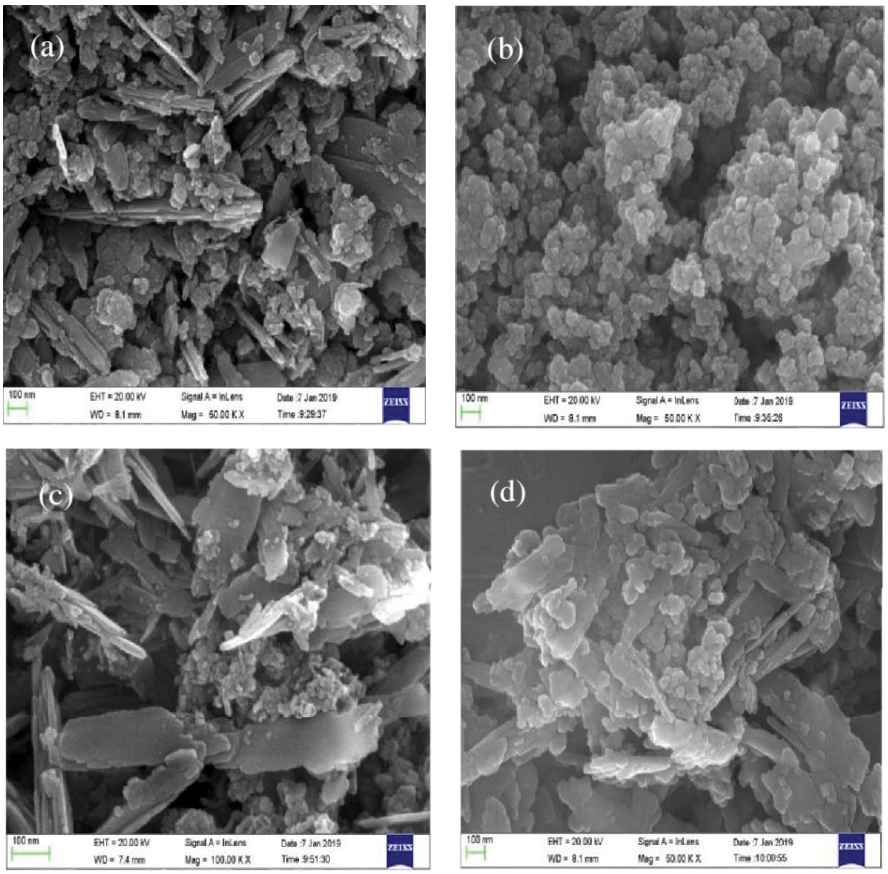

Fig. 10. Scanning electron microscopy of the composite after reacting with different heavy metals: (a) Hg(II), (b) Ag(I), (c) Cd(II), and (d) Pb(II).

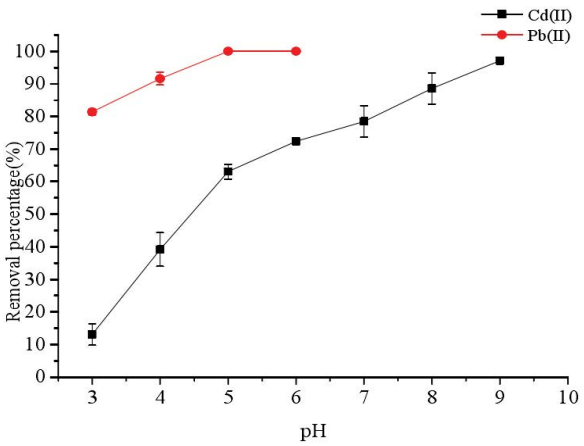

Fig. 11. Effect of initial pH value of the solution on Cd(II) and Pb(II) adsorption rate.

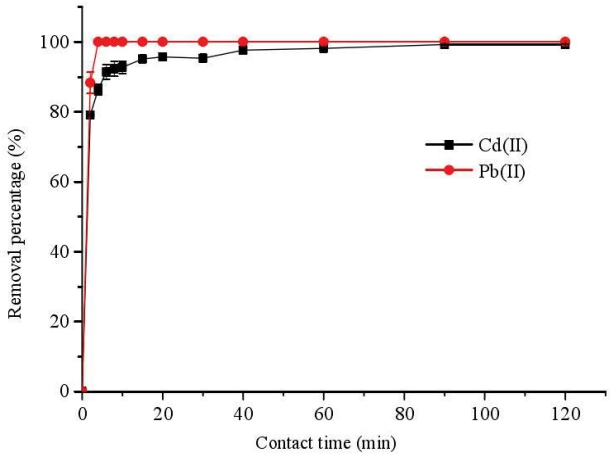

Fig. 12. Curve of adsorption percentage of Cd(II) and Pb(II) in drinking water with time.

can be used to remove trace Cd(II) and Pb(II) in drinking water [24–26].

5. Conclusion

The removal performance of iron oxide for Cd(II) and Pb(II) in an aqueous solution was investigated. The experimental results showed that the removal rates of Cd(II) and Pb(II) in drinking water samples by *in-situ* oxidation of Fe_3O_4 membrane were 99.25% and 100%, respectively, and the treated drinking water met the limits of heavy metals in drinking water stipulated by who. It has great potential in heavy metal remediation.

Acknowledgments

The research is supported by: The science and technology research project "5g+" intelligent network tracking control research based on non-linear artificial intelligence system "of Chongqing Education Commission (subject approval No.: kjqn201903702); research on knowledge co construction of Library discipline and vocational education professional team in the perspective of" artificial intelligence + "of the 13th five year plan of Chongqing Education Science (subject approval No.: 2018-gx-419) Supported by "Research on the effectiveness of deep integration of industry and education" innovation and entrepreneurship "based on undergraduate level vocational schools" sponsored by Chongqing Institute of higher education in 2019–2020 (project approval No.: cqgj19b185); 2016 "Research on social network governance and construction of deep integration of industry and education in Vocational Education" (project approval No.: 1) 6skgh254); research on the system and mechanism of the deep integration of production, teaching and research based on Vocational Undergraduate Education (subject approval No.: 2020zjxh282138); In 2019, the humanities and Social Sciences Research of Chongqing Municipal Education Commission "innovation research of Ideological and political work in Colleges and universities in the era of big data" (subject approval No.: 19sksz101); in 2019, the key scientific research project of Modern Vocational Education Research Institute "Research on the construction of Chongqing Rural Revitalization deep integration social network" (subject approval No.: mverikt201812001).

References

[1] T.C. Nguyen, P. Loganathan, T.V. Nguyen, J. Kandasamy, R. Naidu, S. Vigneswaran, Adsorptive removal of five heavy metals from water using blast furnace slag and fly ash, Environ. Sci. Pollut. Res., 25 (2018) 20430–20438.
[2] M. Chen, K. Shafer-Peltier, S.J. Randtke, E. Peltier, Competitive association of cations with poly (sodium 4-styrenesulfonate) (PSS) and heavy metal removal from water by PSS-assisted ultrafiltration, Chem. Eng. J., 344 (2018) 155–164.
[3] W. Zhang, H. Oswal, J. Renew, K. Ellison, C.-H. Huang, Removal of heavy metals by aged zero-valent iron from flue-gas-desulfurization brine under high salt and temperature conditions, J. Hazard. Mater., 373 (2019) 572–579.
[4] S. Bilardi, P.S. Calabro, R. Greco, N. Moraci, Selective removal of heavy metals from landfill leachate by reactive granular filters, Sci. Total Environ., 644 (2018) 335–341.
[5] P. Yang, L. Yang, Y. Wang, L. Song, J. Yang, G. Chang, An indole-based aerogel for enhanced removal of heavy metals from water via the synergistic effects of complexation and cation–π interactions, J. Mater. Chem. A, 7 (2019) 531–539.
[6] V.B. Yadav, R. Gadi, S. Kalra, Clay based nanocomposites for removal of heavy metals from water: a review, J. Environ. Manage., 232 (2018) 803–817.
[7] W. Ewa, W. Maria, The effect of selected acidic or alkaline chemical agents amendment on leachability of selected heavy metals from sewage sludge, Sci. Total Environ., 633 (2018) 463–469.
[8] L. Joseph, B.M. Jun, J.R.V. Flora, C.M. Pink, Y. Yoon, Removal of heavy metals from water sources in the developing world using low-cost materials: a review, Chemosphere, 229 (2019) 142–159.
[9] K. Zhang, F. Yong, D.T. McCarthy, A. Deletic, Predicting long term removal of heavy metals from porous pavements for stormwater treatment, Water Res., 142 (2018) 236–245.
[10] M.N. Sultana, M.S. Hossain, G.A. Latifar, Water quality assessment of Balu River, Dhaka Bangladesh, Water Conserv. Manage., 3 (2019) 08–10.
[11] A. Maqbool, W. Hui, M.T. Sarwar, Nanotechnology development for *in-situ* remediation of heavy metal (Loid)S contaminated soil, Environ. Ecosyst. Sci., 3 (2019) 09–11.
[12] S. Sharma, S. Upadhyay, B. Singh, Employment opportunities with promoting waste management in India, J. Clean WAS, 3 (2019) 10–15.

[13] M. Shorie, H. Kaur, G. Chadha, K. Singh, P. Sabherwal, Graphitic carbon nitride QDs impregnated biocompatible agarose cartridge for removal of heavy metals from contaminated water samples, J. Hazard. Mater., 367 (2019) 629–638.
[14] M.E. Mahmoud, E.A. Saad, M.A. Soliman, M.S. Abdelwaheb, Removal of radioactive cobalt/zinc and some heavy metals from water using diethylenetriamine/2-pyridinecarboxaldehyde supported on NZVI, Microchem. J., 145 (2019) 1102–1111.
[15] D. Eeshwarasinghe, P. Loganathan, S. Vigneswaran, Simultaneous removal of polycyclic aromatic hydrocarbons and heavy metals from water using granular activated carbon, Chemosphere, 223 (2019) 616–627.
[16] H. Gogoi, T. Leivisk, E. Heiderscheidt, H. Postila, J. Tanskanen, Removal of metals from industrial wastewater and urban runoff by mineral and bio-based sorbents, J. Environ. Manage., 209 (2018) 316–327.
[17] N. Jamil, N. Khan, R. Jabeen, R. Mehmood, N. Naheed, Synthesis, characterisation and applications of new Schiff base as microbicidal agent and removal of heavy metals from water, Int. J. Environ. Anal. Chem., (2019) 1–15, doi: 10.1080/03067319.2019.1694669 (Early Online Version).
[18] P. Fan, X. Jiang, J. Qiao, L. Li, Enhanced removal of heavy metals by zerovalent iron in designed magnetic reactors, Environ. Technol., 39 (2018) 2542–2550.
[19] D. Gounden, S. Khene, N. Nombona, Electroanalytical detection of heavy metals using metallophthalocyanine and silica-coated iron oxide composites, Chem. Pap., 72 (2018) 3043–3056.
[20] S. Mosivand, I. Kazeminezhad, S.P. Fathabad, Easy, fast, and efficient removal of heavy metals from laboratory and real wastewater using electrocrystalized iron nanostructures, Microchem. J., 146 (2019) 534–543.
[21] B. Ranjan, S. Pillai, K. Permaul, S. Singh, Simultaneous removal of heavy metals and cyanate in a wastewater sample using immobilized cyanate hydratase on magnetic-multiwall carbon nanotubes, J. Hazard. Mater., 363 (2019) 73–80.
[22] M. Feng, P. Zhang, H.-C. Zhou, V.K. Sharma, Water-stable metal-organic frameworks for aqueous removal of heavy metals and radionuclides: a review, Chemosphere, 209 (2018) 783–800.
[23] E.-B. Son, K.-M. Poo, J.-S. Chang, K.-Y. Chae, Heavy metal removal from aqueous solutions using engineered magnetic biochars derived from waste marine macro-algal biomass, Sci. Total Environ., 615 (2018) 161–168.
[24] Y. Chen, N. Liu, L. Ye, S. Xiong, S. Yang, A cleaning process for the removal and stabilisation of arsenic from arsenic-rich lead anode slime, J. Cleaner Prod., 176 (2018) 26–35.
[25] J. Liu, Y. Liu, X. Wang, An environmental assessment model of construction and demolition waste based on system dynamics: a case study in Guangzhou, Environ. Sci. Pollut. Res. Int., 27 (2019) 37237–37259.
[26] S. Roy, G. Handique, F.R. Bora, A. Rahman, Evaluation of certain non-conventional plant based oils against red spider mite of tea, J. Environ. Biol., 39 (2018) 1–4.